

Article

Research on Characteristics of Groundwater Recharge in the Weishan Irrigated District Based on a Bromide Tracer

Xin Cong, Zhenghe Xu * and Tong Wang

School of Water Conservancy and Environment, University of Jinan, Jinan 250022, China; congxin1994@126.com (X.C.); 18766125036@163.com (T.W.)

* Correspondence: xu4045@126.com; Tel.: +86-186-6080-9542

Received: 4 May 2018; Accepted: 12 June 2018; Published: 17 June 2018



Abstract: Bromide was used as tracer in the Weishan Irrigated District to determine the groundwater recharge as well as to evaluate the impacts of different irrigation basin locations, irrigation regimes, and crop types on the recharge. The comprehensive recharge coefficient and the Kriging Spatial Interpolation methods were used to distinguish the effects of precipitation and surface water irrigation on the groundwater recharge rate. The results show that the recharge rates ranged from 85.8 to 243 mm/a, with an average of 168 mm/a. The average recharge rate in the upstream district is greater in the downstream and the average recharge rate of irrigated land (193 mm/a) is greater than non-irrigated land (110 mm/a). The recharge rates in fields of winter wheat-summer maize and cotton with irrigation are 210 mm/a and 140 mm/a, respectively, while they are 115 mm/a and 94.1 mm/a under no irrigation conditions. The comprehensive recharge coefficient of groundwater in the upstream irrigation area is larger than that in the downstream. By comparing the spatial distribution of the groundwater level and the comprehensive recharge coefficient, it is found that there is a positive relationship between the groundwater level and the comprehensive recharge coefficient. The results of this study can provide reference and guidance to a water resources analysis of the Weishan Irrigated District.

Keywords: bromide; tracer method; the Weishan Irrigated District; groundwater recharge; recharge rate

1. Introduction

Groundwater recharge is a basic component of the groundwater system [1]. The groundwater system of the irrigated district belongs to the half-natural system, as well as the water cycle, which is more complex due to the influence of human activities [2,3]. With the rapid development of industry and agriculture, the contradiction between the supply and demand of water is prominent in the day to day; however, less attention is devoted to recognizing the characteristics of groundwater supply, runoff, and drainage, which results in the phenomena of ground subsidence, brackish water, and saltwater intrusion [4,5]. The objective of this research is to find out the characteristics of groundwater recharge in the irrigation area, providing a theoretical basis for the scientific, rational utilization, and deployment of groundwater resources that can manage the stable and healthy development of irrigation areas.

The hydrogeological parameters are an indispensable data source for solving hydrogeological calculations. One of the most important parameters is the recharge rate, which is often difficult to determine by conventional methods. Since the mid-80s of the last century, researchers have been using different methods to study groundwater recharge mechanisms [6,7]. There are four methods that are most influential and representative [8–10]: Physical Method (the water-balance, water table fluctuation),

Chemical Tracer Method, Lysimeter, and Numerical Simulation Methods. The spatial-temporal variations of groundwater are complicated, which make methods such as the Lysimeter and Physical Method less efficient in discovering the evolutionary characteristics of groundwater recharge in a study area [11,12]. In comparison to these methods, the Artificial Tracer method has the advantage of not requiring a large volume of hydrological data and it obtains data more easily. Thus, it is usually chosen to estimate groundwater recharge and simultaneously determine the recharge sources, the flow speed, migration time, and to identify the preferred flow paths [13–15]. In addition, the artificial tracer has the characteristic of wide selectivity; any material with properties of high water solubility, chemical stability, low environmental pollution, simple measurement, high precision, low testing expense, etc., can be used as a tracer.

The Artificial Tracer method is consistently used in various types of hydrological and hydrogeological environments to attain information about water movement and contaminant transport. Dravis et al. [16] found the source of pollutants in the water of the study area by using sulfur hexafluoride as a tracer in a large-scale test over the study area. Hulla et al. [17] used tracer methods in Slovakia to check deep excavation sealing element efficiency, which was significant for protecting water resources from radioactive contamination. While estimating the recharge rate and discharge rate have relied to a large extent on tracer (neon, bromide, chloride, and tritium) profiles, many radioisotopes were used to estimate the flow rates [18]. Sukhija et al. [19] used an artificial and geochemical tracer to estimate the intake area of a confined aquifer and the recharge rates of the intake area, thus calculating the amount of recharge by direct precipitation to the confined aquifer. Therefore, researchers have adopted an artificial tracer method to study the correlation characteristics of groundwater recharge for a long time. Zimmermann et al. [20] pioneered the use of neon as a tracer to study soil water transport. Neon was widely used as an applied tracer [21–23]. Afterwards, many researchers used bromide as a tracer to study soil solute transport [24–26]. Flint et al. [27] used bromide to procure a better understanding of the movement and transport of water through the soil profile. However, it was rare to use a bromine tracer to study groundwater recharge. Rice et al. [28] used a bromine tracer technique to evaluate the recharge rate of bare land under rainfall and irrigation conditions (45 cm). These studies usually put tracers on the surface, which reduces the reliability of the evaluation results. Subsequently, artificial tracers were put to the surface or underground at a certain depth, which could overcome the effects of the soil roots and large voids. Rangarajan et al. [29] analyzed the recharge rate of several basins and watersheds in India by the tritium injection method, which showed the recharge rate ranged from 24 to 198 mm year^{−1} or 4.1 to 19.7% of the local average seasonal rainfall. Multiple age tracers were measured to estimate groundwater residence times in the regional aquifer system underlying southwestern Oman, which proved that the age of the confined groundwater was longer in the Dhofar Mountains [30]. WU et al. [31] and Tan et al. [32] took the North China Plain and the Central Plain as an example, using the tracer method to study the groundwater recharge under the conditions of irrigation and non-irrigation.

The main objectives of this study are to (1) evaluate the influence of different irrigation district locations, irrigation regimes, and crop types on the groundwater recharge in the Weishan Irrigated District; (2) establish the relationship between the groundwater recharge and the irrigation and rainfall; and (3) develop the relationship between the groundwater level and the comprehensive recharge coefficient.

2. Materials and Methods

2.1. Study Area

The Weishan Irrigated District, the largest in the Yellow River irrigation area in the lower reaches of the Yellow River, is located in Liaocheng City, Shandong Province (Figure 1a). It extends from 113° E to 118° E longitude and 34° N to 36° N latitude with a total area of 5400 km². The scale of the irrigation area ranks fifth in the whole country, 3600 km² of which is a designated and designed irrigation area.

The Tuhai River and Majia River pass through from the middle of the irrigation area. Irrigation and precipitation are the main sources of recharge through the shallow groundwater.

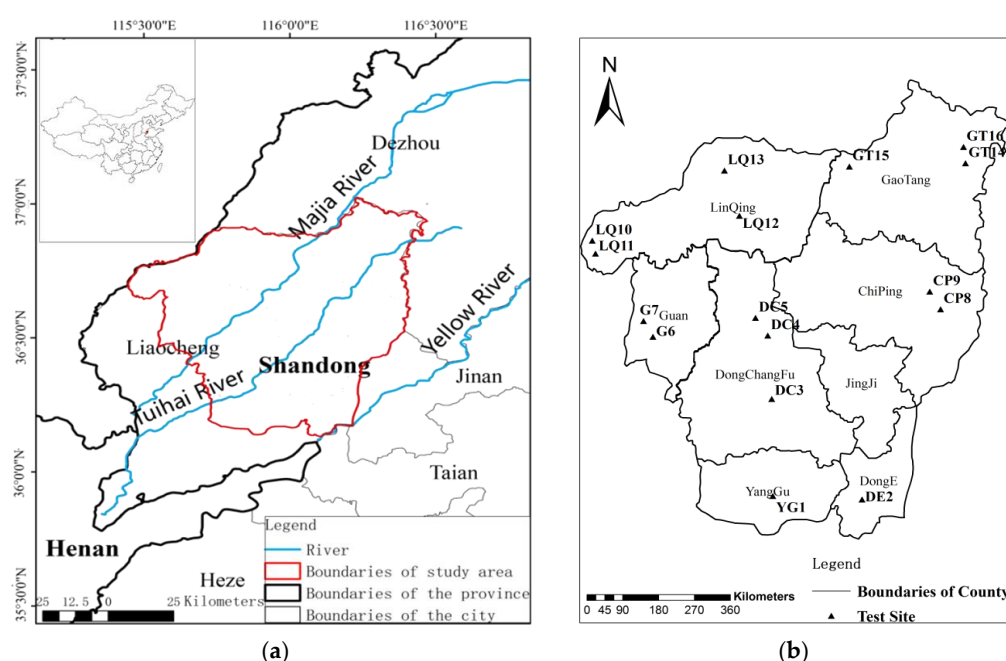


Figure 1. Location of the (a) study area and (b) sampling points and tracer injection.

In this experiment, the tracer test area was selected by the preliminary investigation. The precipitation concentrated on the flood season (June–September), and the irrigation water concentrated in two periods, or the period from March to May and the period from September to November in the research area. Considering the effects of precipitation and irrigation on the movement of bromine tracers, before the irrigation begins the bromide was injected during 9–11 February 2015. The flood season was divided into two stages and the first sampling time was selected on 25–29 July 2015. The second sampling time was selected on 3–7 May 2016 when the irrigation ended. According to the attributes of the testing site, such as spatial location, irrigation, crop planting and so on, a total of 16 sampling points in seven representative sites (i.e., the Dongchangfu (DC), Linqing (LQ), Yanggu (YG), Chiping (CP), Donge (DE), Guan (G), and Gaotang (GT) sites) were selected for particular research (Table 1 and Figure 1b). However, among them 2 sampling points were abandoned due to the construction of houses and roads. General features of the sampling points are listed in Table 1.

Table 1. Summary of bromide sampling points.

Administrative Areas	Sampling Number	Irrigation Regime		Crop Types		
		Non-Irrigated Land	Irrigated Land	Winter Wheat-Summer Maize	Cotton	Other Types *
Dongchangfu	3	DC4	DC3, DC5	DC4, DC5		DC3
Linqing	4	LQ11, LQ12	LQ10, LQ13	LQ10, LQ12	LQ13	LQ11
Yanggu	1		YG1	YG1		
Chiping	2	CP8	CP9	CP8, CP9		
Donge	1		DE2	DE2		
Guan	2	G6	G7	G6, G7		
Gaotang	3	GT15	GT14, GT16	GT14, GT16	GT15	
Total	16	6	10	12	2	2

Note: * Other types mainly include woodland, wasteland etc.

2.2. Principles and Methods of Bromide Tracer

2.2.1. Principles of Bromide Tracer

The principles for determining groundwater recharge by tracers is as follows: put in tracers at a known depth under natural conditions. The tracer will move downward with the precipitation and irrigation water. Because of the different velocity of tracer movement, tracer enrichment will occur under different conditions. The samples were taken regularly to determine the downward rate of mass concentration of tracer in profile and soil moisture so as to finally calculate the recharge rate of the groundwater. The principles are shown in Figure 2. After a certain period of time, samples are collected to monitor the change of tracer concentration in the section, and then the groundwater recharge rate is calculated by observing the downward movement of the tracer peak with the following equation [33]

$$R_r = v \times \theta = \frac{\theta \times \Delta Z}{\Delta t} \quad (1)$$

where, R_r is the recharge rate (mm/day); v is the vertical infiltrating velocity of soil water (mm/day); Δt is the time between tracer injection and sampling (day); ΔZ is the depth of tracer peak (mm); and θ is the average soil moisture content within the depth interval ΔZ during Δt .

The comprehensive recharge coefficient (R_c) is used to study the intensity of the precipitation or irrigation entering into the groundwater, which can be described as

$$R_c = \frac{R_r \times \Delta t}{P + I} \times 100\% \quad (2)$$

where, R_c is the comprehensive recharge coefficient (%); R_r is the recharge rate (mm/day); P is precipitation during Δt , (mm); and I is irrigation during Δt , (mm).

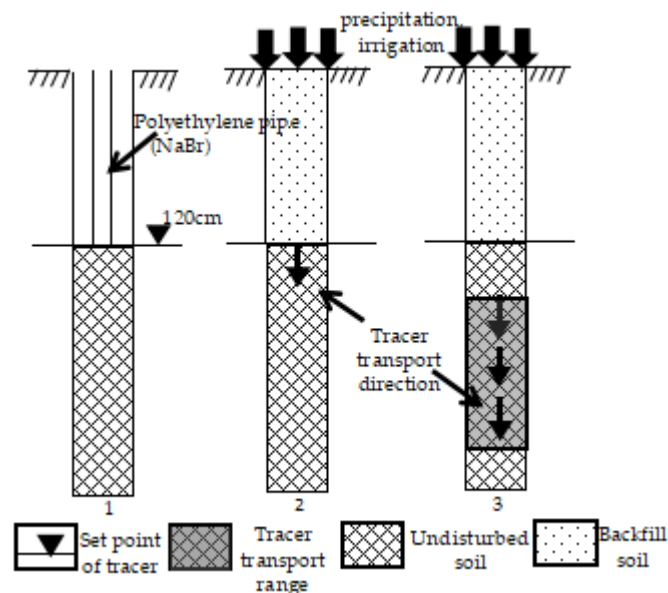


Figure 2. The principles diagram of the tracer experiment.

2.2.2. Methods of Bromide Tracer

To ensure a relatively uniform tracer mass concentration distribution at the different depths of the tracer, a tracer was injected using a porous deep injection method, as shown in Figure 3. Three holes (2 cm in diameter and 120 cm deep) at the vertices of a 30 cm equilateral triangle were drilled with a sampler for bromine injecting. The hole forming was carried out by using a Luoyang shovel. We put the Luoyang shovel into the inside of the polyethylene pipe and the pipe was also brought

into the underground by the Luoyang shovel. The polyethylene pipe was used as a conduit for the injection of bromine tracers. 50 g NaBr (the bromide tracer) was injected at the holes through a conduit. Finally, the pipe was removed from the underground at intervals of 5 cm, then buried with raw soil and subjected to soil compaction. Multiple sampling can be collected near the midpoint of the three injecting points, but did not repeat the sampling points last time.

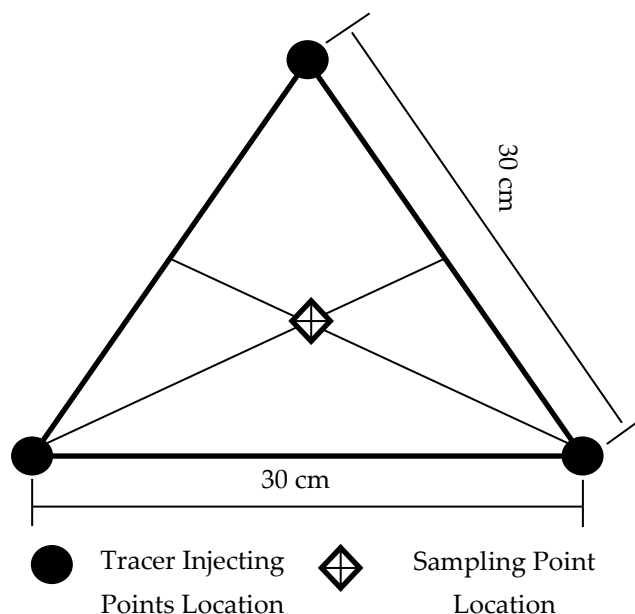


Figure 3. Schematic figure of sampling and tracer injecting points location.

2.3. Analysis Methods

(1) Soil Sampling

At each sampling point, soil samples at different depths (0–4.0 m) were collected by an undisturbed soil sampler. The sampling depth intervals were 20 cm from 0 m to 1.2 m and 10 cm from 1.2 m to 4.0 m. Each soil sample was stored in a plastic bag to minimize evaporation and the weight of fresh soil samples was measured using portable electronic balances.

(2) Moisture Content

Moisture content was measured by the oven drying method. As soon as the samples were sent to the laboratory, the soil samples for measuring the soil moisture content were put into an oven at 105 °C for 24 h. After drying, the weight of the soil was measured by electronic balance, and then the soil water content was obtained by conversion.

(3) Bromide Concentration

The bromide concentration was measured by an ion electrode method (Model: Rex PBr-1-01; Manufacturer: BeijingTongRunYuan Electromechanical Technology Co Ltd., Beijing, China). Briefly, 100 mL of deionized water was added to 20 g of drying sample and shaken for 3 h. Then the mixture was placed to separate into layers. The resulting solution was filtered through a filter and stored in a polyethylene bottle until analysis.

2.4. Statistical Analysis

The recharge characteristics of groundwater under different factors were analyzed by maintaining other effect factors constant. The linear correlation analysis was carried out to study the relationship between the irrigation or precipitation and the recharge rate. The relationship between the groundwater

level and the comprehensive recharge coefficient was analyzed using the Kriging Spatial Interpolation method [34].

3. Results and Discussion

3.1. Bromide Concentration and Moisture Content in the Typical Sites

According to the condition of precipitation data and field irrigation, four typical sites were selected, which were the irrigated district (YG1) and non-irrigated district (DC4) in the upstream; and the irrigation district (GT14) and non-irrigated district (GT15) in the downstream. The determination results are shown in Table 2 and Figure 4.

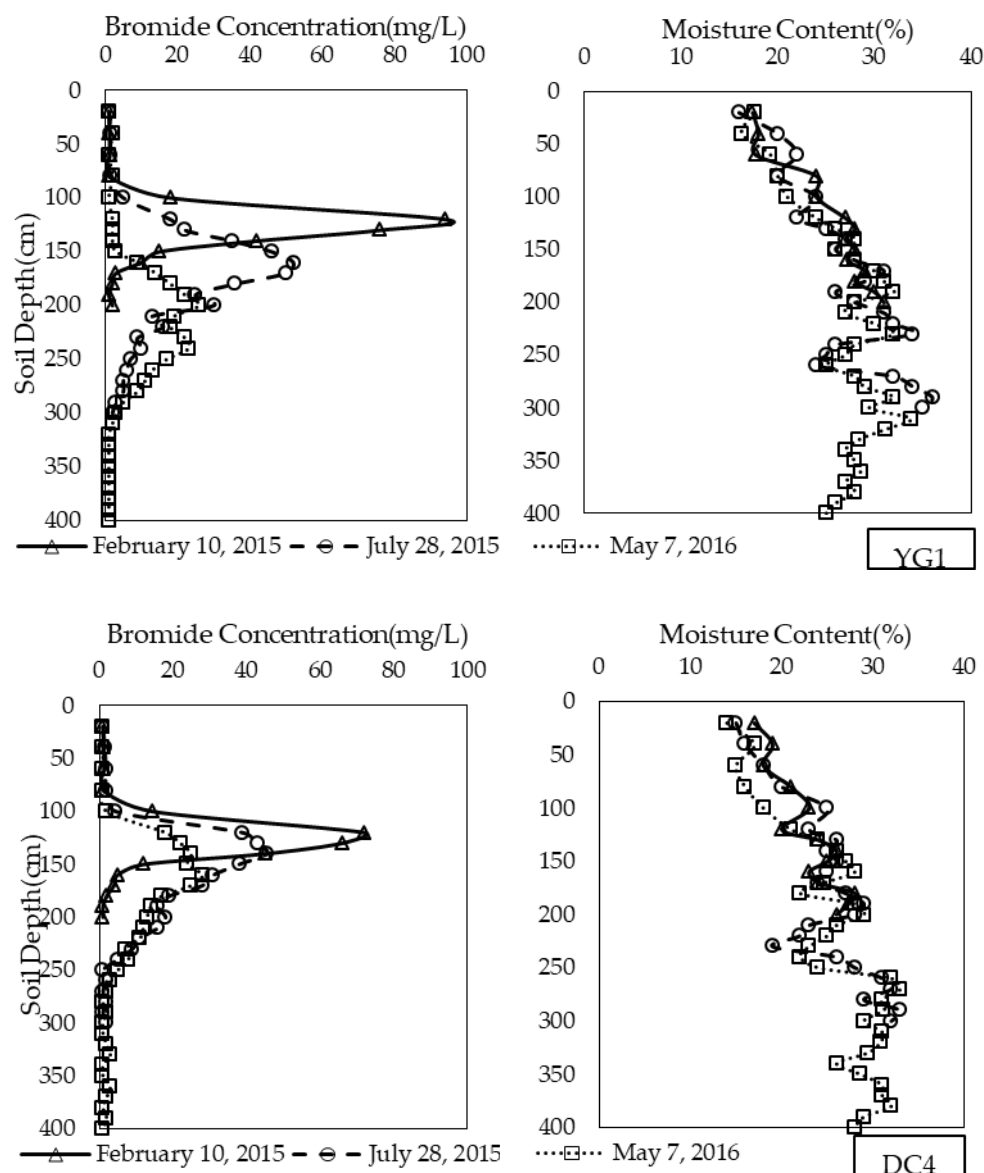


Figure 4. Cont.

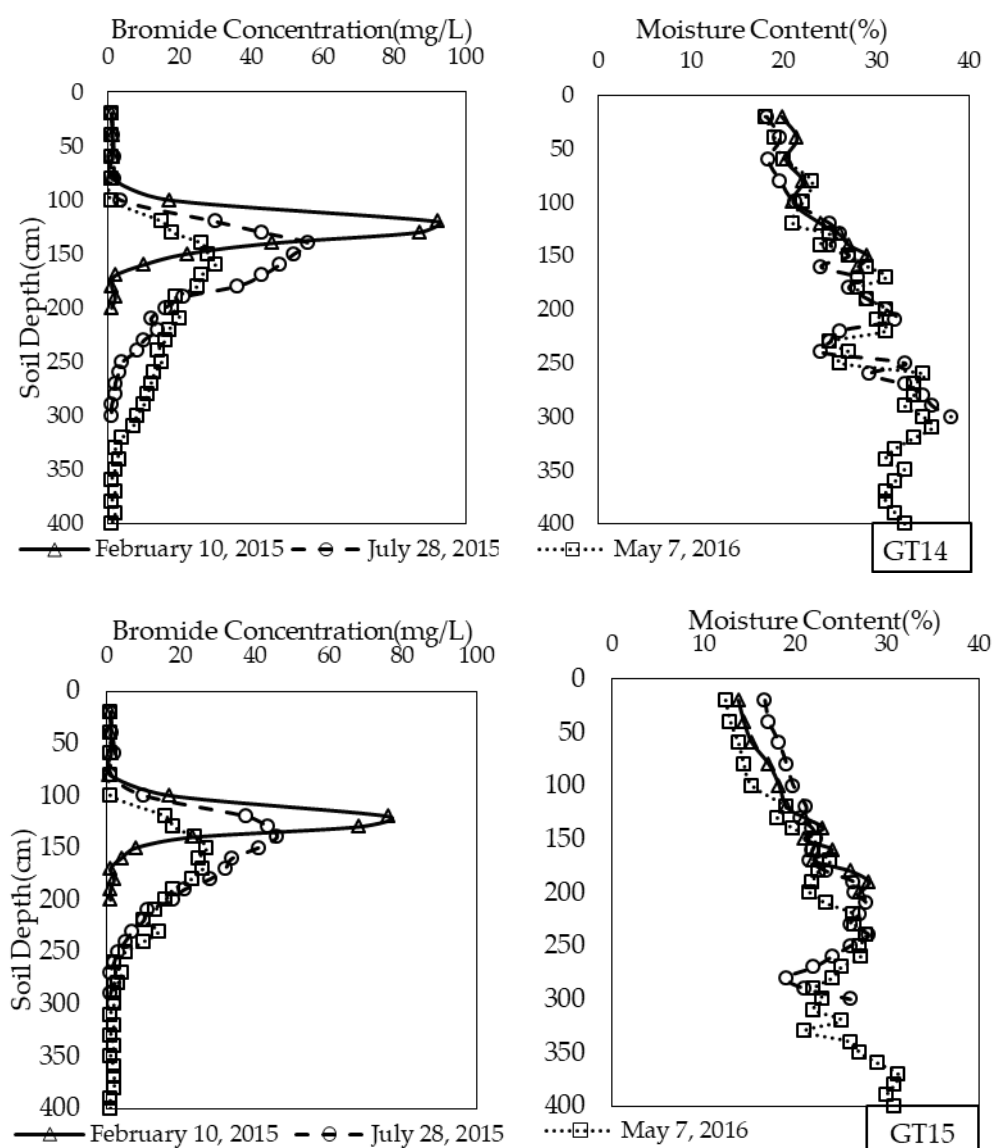


Figure 4. Bromide concentration and moisture content in typical sites.

From Figure 4 it can be seen that the downward movement of the tracer peaks was determined by the shape of the curve from the profiles, the largest value of tracer concentration. The unimodal shape of the bromine concentration curve is consistent with most studies. Bromide concentration distribution varies considerably at different depths, and has a peak that moves downward gradually with increasing time. Moreover, the velocity of bromine in an irrigation area is greater than that in a non-irrigated area. In the same position, from the two sampling bromine concentration curve and table, we can see that the peak value and the depths of the peak value in GT14 with irrigation were larger than that in GT15 without irrigation.

The inter-annual change trends of soil moisture content at each site are similar, with no significant change and showing a similar distribution. The soil moisture content in the irrigation area is larger than that in the non-irrigated area, while the difference of soil moisture content for deep soils was smaller.

Table 2. Summary of recharge determined by bromide concentration in typical sites unit: mg/L.

Depth	YG1			DC4			GT14			GT15		
	10 February 2015	28 July 2015	7 May 2016	10 February 2015	28 July 2015	7 May 2016	10 February 2015	28 July 2015	7 May 2016	10 February 2015	28 July 2015	7 May 2016
20	1.01	1.12	1.33	1.01	1.35	1.00	1.00	1.03	1.01	1.00	1.08	1.00
40	1.21	1.52	2.03	1.16	1.55	1.25	1.21	1.43	1.03	1.11	1.50	1.03
60	1.32	1.34	1.04	1.25	1.80	1.26	1.33	1.56	1.00	1.22	1.98	1.03
80	1.00	1.34	2.03	1.00	1.94	1.27	1.00	1.78	1.54	1.00	1.02	1.03
100	18.36	5.24	2.11	14.50	4.56	2.01	17.24	3.34	1.78	17.21	9.97	1.95
120	94.58	18.05	2.13	72.36	39.20	18.36	92.35	30.01	15.21	75.91	37.69	15.98
130	76.86	22.11	2.18	66.58	43.58	22.12	87.47	43.21	17.95	68.04	43.50	18.32
140	42.39	35.06	2.19	45.32	45.48	25.03	45.96	56.24	26.21	22.87	46.13	23.95
150	15.13	46.07	3.21	12.12	38.35	24.21	22.12	51.98	28.22	8.14	40.95	27.03
160	10.25	52.04	9.06	5.02	31.25	28.18	9.98	47.86	29.69	3.94	34.15	25.32
170	3.01	50.01	14.53	4.21	28.21	25.00	1.95	43.05	25.34	1.12	32.56	25.98
180	2.04	36.24	18.32	2.01	19.32	17.18	1.22	35.87	24.98	1.97	28.88	23.04
190	1.02	25.11	22.14	1.05	16.12	14.57	2.00	21.52	19.02	1.13	21.21	18.55
200	2.07	30.03	26.52	1.01	18.20	13.24	1.03	16.45	17.87	1.05	17.89	16.35
210	-	13.12	19.03	-	16.05	11.96	-	12.06	19.94	-	11.21	13.21
220	-	16.08	18.00	-	11.13	10.87	-	13.98	17.15	-	9.93	9.86
230	-	9.01	22.01	-	8.98	7.08	-	9.99	16.24	-	7.11	14.23
240	-	10.12	23.00	-	5.22	7.99	-	8.04	13.92	-	4.92	9.96
250	-	7.21	17.21	-	1.00	5.12	-	4.06	14.35	-	2.87	5.06
260	-	6.10	13.12	-	1.89	2.99	-	3.03	13.22	-	1.98	2.32
270	-	5.01	11.01	-	1.00	2.02	-	1.97	12.00	-	1.02	4.21
280	-	5.01	9.06	-	1.75	1.00	-	1.85	11.32	-	1.98	3.22
290	-	3.03	5.21	-	1.00	2.11	-	1.00	10.00	-	1.03	1.99
300	-	2.04	3.11	-	2.01	1.00	-	1.00	8.35	-	1.86	1.98
310	-	-	2.03	-	-	1.00	-	-	7.21	-	-	1.00
320	-	-	1.06	-	-	2.03	-	-	4.05	-	-	2.01
330	-	-	1.06	-	-	2.99	-	-	2.12	-	-	1.04
340	-	-	1.04	-	-	1.00	-	-	2.99	-	-	1.98
350	-	-	1.04	-	-	1.00	-	-	2.03	-	-	1.08
360	-	-	1.02	-	-	2.89	-	-	1.24	-	-	1.86
370	-	-	1.02	-	-	2.01	-	-	1.97	-	-	1.85
380	-	-	1.02	-	-	1.32	-	-	1.02	-	-	1.83
390	-	-	1.02	-	-	1.96	-	-	1.89	-	-	1.02
400	-	-	1.02	-	-	1.00	-	-	1.03	-	-	1.01

3.2. The Recharge Rate

The annual recharge rate for different sites and time in the Weishan Irrigated District is determined by Equation (1) based on the tracing test, which is shown in Table 3 and Figure 5.

Table 3. The recharge rate of groundwater.

Sampling Points	February 2015 to July 2016				July 2015 to May 2016			
	ΔZ (cm)	θ (%)	R_d (mm/Day)	R_a (mm/a)	ΔZ (cm)	θ (%)	R_d (mm/Day)	R_a (mm/a)
YG1	40	34.5	0.81	297	40	38.5	0.54	197
DE2	30	36.4	0.64	235	50	39.4	0.69	251
DC3	40	32.6	0.77	282	30	36.6	0.41	151
DC4	20	30.8	0.36	133	20	38.8	0.29	107
DC5	40	32.7	0.77	283	40	36.7	0.55	202
G6	20	30.9	0.36	133	20	37.9	0.27	97.0
G7	30	34.5	0.61	222	40	39.5	0.55	202
CP9	30	31.7	0.56	204	30	38.7	0.41	148
LQ10	30	32.6	0.59	214	40	36.6	0.52	189
LQ12	20	29.8	0.36	130	20	34.8	0.25	90.0
LQ13	20	30.1	0.36	132	30	38.1	0.4	147
GT14	30	32.5	0.58	212	30	36.5	0.39	141
GT15	20	31.8	0.38	138	10	38.8	0.14	50.0
GT16	20	30.9	0.37	134	30	37.9	0.4	146

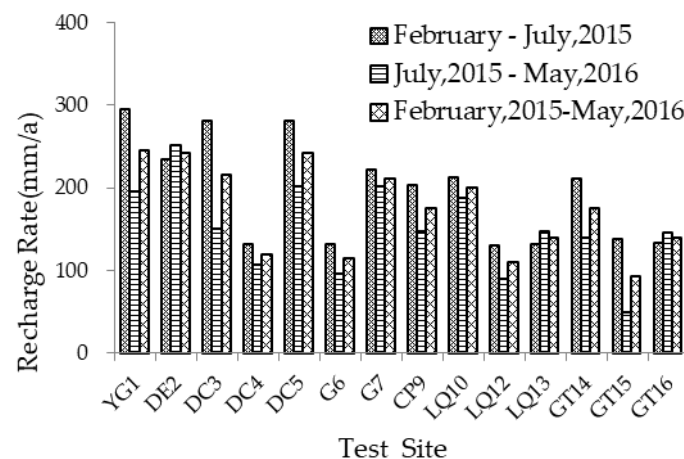


Figure 5. The recharge rate of groundwater in different periods.

It can be seen that the annual recharge rate from 2015 to 2016 was 85.5–243 mm/a (0.23–0.66 mm/day), with an average in different sites of 168 mm/a. The recharge rates were influenced by the irrigation district location, irrigation type, and crop type.

3.2.1. Effect of Irrigation District Locations

Conditions of YG1, DE2, DC5, CP9, GT14, and GT16 (irrigation, winter wheat-summer maize) were almost the same except the irrigation district location. The recharge rates of YG1 and DE2, (upstream district) were 246 mm/a and 243 mm/a, respectively. The recharge rates of DC5, CP9 (midstream) were 242 mm/a and 177 mm/a, respectively. The recharge rates of DT14 and DT16 (downstream) were 176 mm/a and 140 mm/a, respectively. The results showed that the recharge rates for upstream irrigated cropland were greater than those for downstream irrigated cropland. The same was true for sites with non-irrigation and the same crops (DC4 and LQ12 as shown in Figure 6). Underpinning this phenomenon is that the soil texture in the upstream district was much coarser than in the downstream, resulting in more rainfall and irrigation water infiltrated into the

underground. The conclusion agreed with Vucic's view that coarse soil results in more groundwater recharge [35].

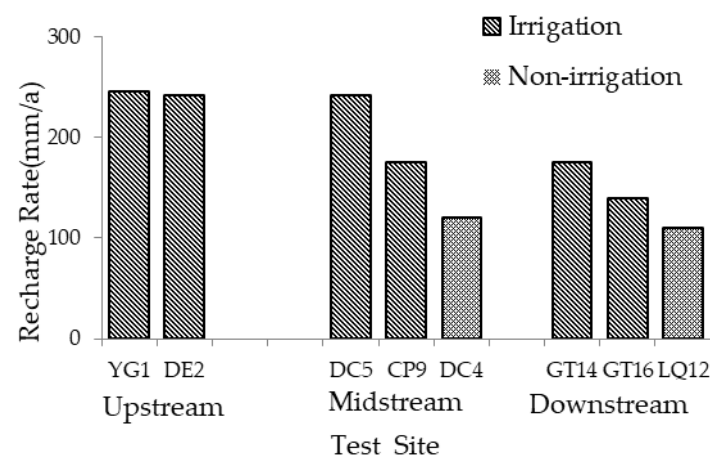


Figure 6. The recharge rate of groundwater in different irrigated district location.

3.2.2. Effect of Irrigation Regime

In the two-year experiment, a comparison of the paired locations (DC5 and DC4, G7 and G6, DT14 and LQ12, LQ13 and GT15) that had nearly the same irrigation district location and crop types showed that there was generally a greater recharge in irrigated lands (DC5, G7, DT14, and LQ13, with an average of 192.5 mm/a) than in non-irrigated lands (DC4, G6, LQ12 and GT15, with an average of 109.7 mm/a) (Figure 7). It is indicated that the utilization rate of irrigation water in irrigated cropland was low and a considerable quantity of irrigation water seeped in to recharge the groundwater. The results show that recharge rates for irrigated cropland were greater than for non-irrigated, non-cultivated land, probably because less irrigation water was absorbed by crop and more irrigation water recharged to the groundwater in the form of irrigation return flow. The results in this study are consistent with those of Wang et al. [10]. The existence of this phenomenon is mainly related to current irrigation methods, such as flood irrigation and other large scale irrigation methods. Therefore, to increase the utilization efficiency of irrigation water and reduce the ineffective consumption of water resources, the sprinkler irrigation technique, which has the advantages of saving water, should be widely used in farmland irrigation.

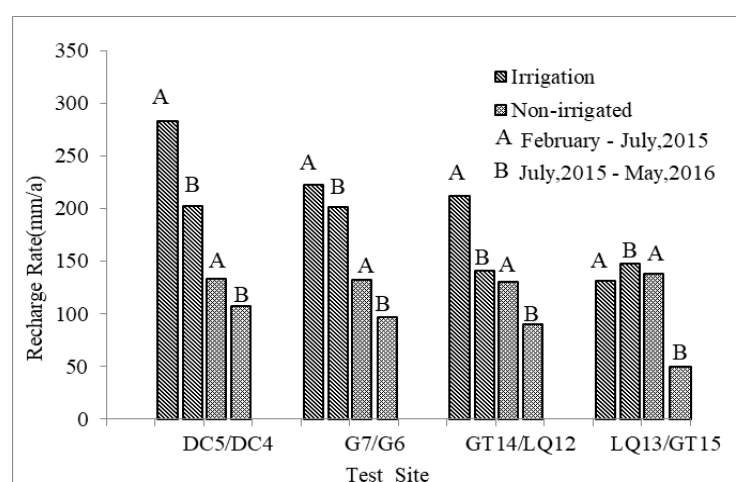


Figure 7. The recharge rate of groundwater in different periods in irrigated cropland and non-irrigated land.

3.2.3. Effect of Crop Types

The influence of different crops on the recharge rate was analyzed by comparing the groundwater recharge rate of irrigation and the non-irrigation testing sites. From Figure 7, it appeared that the recharge rate of winter wheat-summer maize (the first three groups) was higher than those of cotton (the fourth group). The recharge rate of the two crops under an irrigation condition was 210 mm/a and 140 mm/a, respectively, and was 115 mm/a and 94.1 mm/a under a non-irrigation condition. It can be concluded that the soil water use efficiency of cotton was greater than that of winter wheat-summer maize. This may result from the fact that cotton had a larger root length density and consumed more soil water than winter wheat-summer maize [36,37].

3.3. Comprehensive Recharge Coefficient Analysis

3.3.1. Relationship between Recharge Coefficient and Precipitation and Irrigation

We used the calibrated groundwater numerical model to simulate the groundwater recharge in 2015. The results are shown in Table 4.

Table 4. Simulation results of groundwater recharge in 2015.

Month	Supply Source					
	Precipitation and Surface Water Irrigation (10^4 m^3)	Percentage	Accretion Volume of River (10^4 m^3)	Percentage	Lateral Groundwater Recharge (10^4 m^3)	Percentage
1	1593.1	2.0%	73.5	4.3%	6.3	5.3%
2	6303.4	8.0%	85.3	5.0%	5.5	4.6%
3	5753	7.3%	103.5	6.1%	4.5	3.8%
4	7236	9.1%	125.4	7.4%	5.2	4.4%
5	8437.6	10.7%	154.7	9.2%	6.6	5.6%
6	3628.5	4.6%	136.6	8.1%	7.9	6.7%
7	9538.8	12.0%	186.6	11.0%	9.2	7.8%
8	20,214.9	25.5%	267.5	15.8%	13.8	11.6%
9	8335.9	10.5%	234.2	13.9%	20.9	17.6%
10	1516.6	1.9%	145.3	8.6%	18.5	15.6%
11	6120.2	7.7%	103.4	6.1%	13.5	11.4%
12	534.6	0.7%	74.3	4.4%	6.6	5.6%
Sum	79,212.7		1690.1		118.6	
Percentage	0.978%		0.021%		0.001%	

Note: the total amount of groundwater recharge includes the storage capacity of aquifer.

From the view of the supply source, the table shows that precipitation and irrigation are an important part of groundwater recharge, which shared about 76.5 percent of the total amount of recharge. From the view of the supply time, the key periods were the flood season and irrigation period. We could draw a conclusion that the groundwater recharge was affected by precipitation and irrigation, and the two factors cannot be distinguished. This conclusion agrees with the views of Allocca et al. [38] and Owor et al. [39]. Thus, the comprehensive recharge coefficient was adopted to determine the spatial distribution characteristics of the groundwater recharge rate in the irrigation area, which can separate the atmospheric precipitation from the infiltration coefficient. According to the average result of bromide tracing, the effects of precipitation or irrigation on the recharge were quantitatively analyzed. There was a linear relationship between the groundwater recharge and the precipitation and irrigation ($R^2 = 0.7526$, $P < 0.05$), which is shown in Figure 8. The linear relationship by the least-squares fitting was $R = 0.1897 (P + I) + 1.8965$, where R is the comprehensive recharge coefficient (mm/a), P is the precipitation (mm), and I is the irrigation (mm).

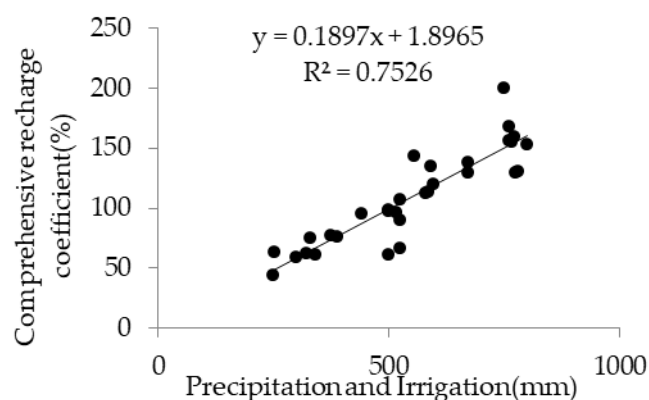


Figure 8. Recharge versus precipitation and irrigation.

3.3.2. Spatial Variability of Recharge Coefficients

The precipitation data was provided by the Liaocheng Hydrological Bureau, and the amount of surface water irrigation was obtained through investigation. The investigation indicated that the cropland irrigation had all adopted a border irrigation with an irrigation quota of 80 m³ for farmland; however, the irrigation quota was relatively small for orchards. Four irrigations were carried out each year between March to May and September to October, so from February 2015 to July 2015, the irrigation water amount was 240 mm for farmland and 180 mm for orchard. According to the tracer test results, the comprehensive recharge coefficient of each testing site was calculated during different testing periods (Table 5 and Figure 9).

Table 5. The recharge coefficient of groundwater.

Sampling Points	February 2015 to July 2015			July 2015 to May 2016		
	<i>P</i> (mm)	<i>P</i> + <i>I</i> (mm)	<i>R_c</i> (%)	<i>P</i> (mm)	<i>P</i> + <i>I</i> (mm)	<i>R_c</i> (%)
YG1	328	543	25.4	361	768	20.1
DE2	349	571	19.1	384	780	25.2
DC3	337	644	20.2	370	529	20.8
DC4	334	334	18.4	369	369	21
DC 5	335	574	22.8	371	789	18.6
G6	315	315	19.6	317	317	23.9
G7	312	455	22.8	335	757	20.9
CP9	342	536	17.7	371	766	15.2
LQ10	312	497	19.7	349	761	19.2
LQ 12	297	297	20.1	381	381	18.3
LQ 13	294	497	12.1	334	661	17.3
GT14	267	515	18.9	272	561	19.5
GT15	265	265	24	261	261	14.9
GT16	269	515	12	276	741	15.4

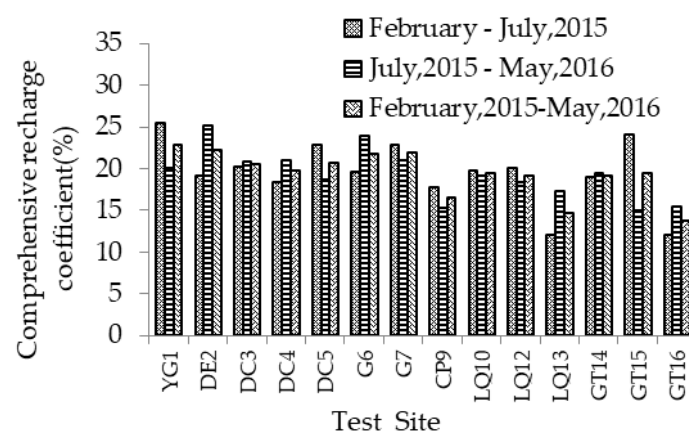


Figure 9. The recharge coefficient of groundwater in different periods.

The average recharge rate determined by bromide tracing tests for different sites varied from 12.0–25.4% and 14.9–25.2%, with the average of 19.5% and 19.3%, respectively. From Table 3 and Figure 9 it can be seen that the recharge rates changed with the location, irrigation regimes, and crop cultivation. The irrigated cropland with winter wheat-summer maize in the upstream (YG1) showed the highest recharge rate. The recharge rate of winter wheat-summer maize fields with irrigation (LQ12, DC5) was higher than that of cotton fields with irrigation (LQ13) and cropland with non-irrigation (DC4) in the same location.

The experimental data were spatially interpolated by Kriging Spatial Interpolation methods to analyze the spatial distribution of the groundwater recharge characteristics in the Weishan Irrigated District, with the results shown in Figure 10.

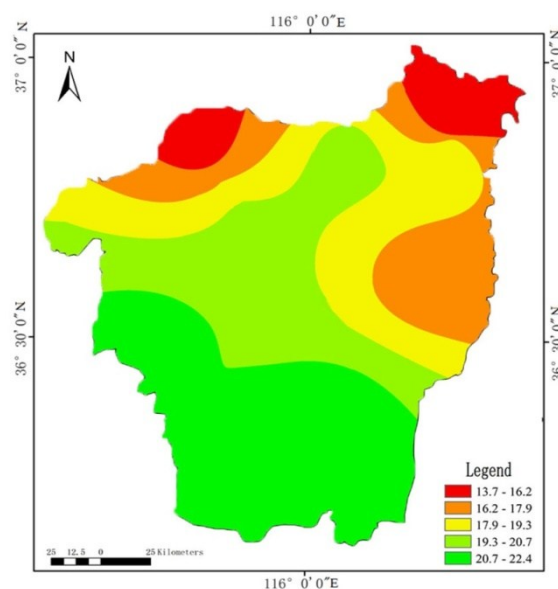


Figure 10. Spatial distribution map of comprehensive recharge coefficient.

From Figure 10 and Table 3 it can be seen that the comprehensive recharge coefficient in the upstream district was larger than in the downstream, which ranged from 20.7% to 22.4% in Yanggu, Dong'e and Liaocheng, and from 13.7% to 16.2% in Linqing and Gaotang. This is because the amount of surface water irrigation in the upstream irrigation district is larger than in the downstream. The other reason is the higher utilization rate of groundwater in the downstream, which is because the soil texture is mostly clay and sandy loam and the crops are mainly cotton.

3.3.3. Analysis of Influencing Factors

The difference in precipitation, as well as aquifer lithology and crops lead to the difference in groundwater recharge produced by precipitation. In the study area, the amount of irrigation water decreased gradually from the upstream to the downstream, which resulted in the spatial difference of groundwater recharge produced by irrigation. Moreover, we supposed that the groundwater recharge was also affected by the depth of the groundwater level. Therefore, based on the measured data from the shallow groundwater level view logging in the irrigation area, the spatial difference of the groundwater level was carried out by Kriging Spatial Interpolation methods in the irrigation district, as shown in Figure 11a.

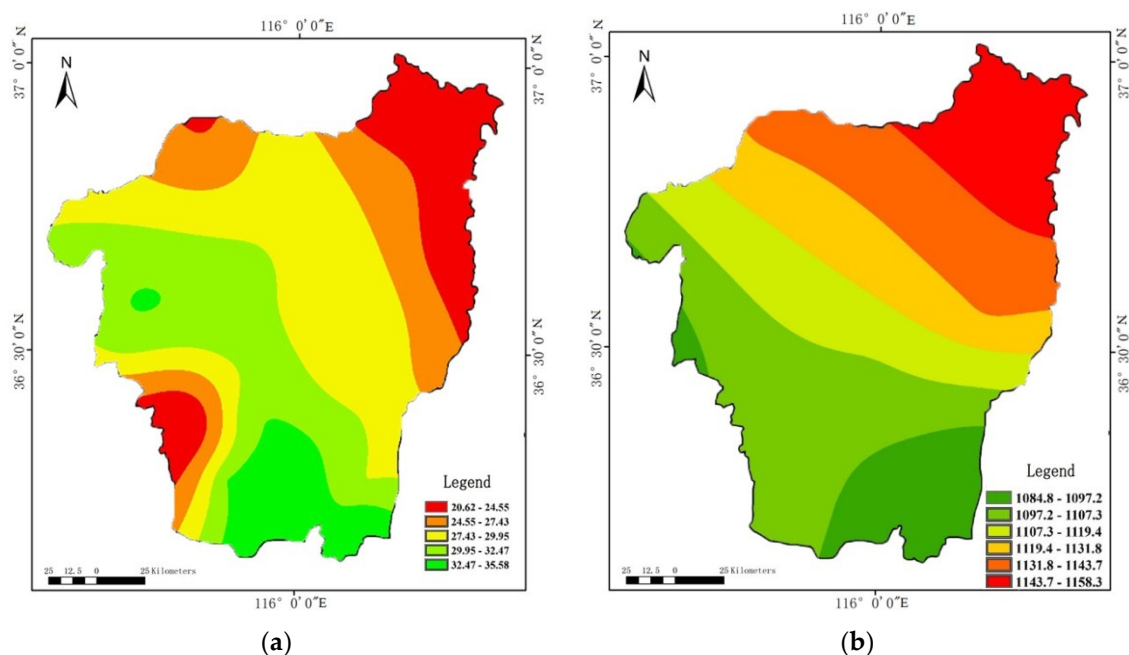


Figure 11. Spatial distribution map of (a) groundwater level and (b) evapotranspiration.

From this, we obtained the data about the groundwater level at each sampling point (Figure 12). A certain positive correlation was found between the groundwater level and the comprehensive recharge coefficient (Figure 13), which was consistent with Meng's conclusion [40]. It can be seen that the recharge coefficient increased with the level at the higher groundwater level, but the correlation between the two was no longer obvious at the lower groundwater level. This conclusion agreed with the views of Tan et al. [32]. The reason of this phenomenon was worth further research. Thus, the evaporation capacity data were spatially interpolated by Kriging Spatial Interpolation methods to plot the spatial distribution map of the evapotranspiration, with the results shown in Figure 11b. It was found that the amount of evaporation was relatively large in the area where the groundwater level was deep and the amount of groundwater recharge was relatively small, which conformed with the phenomenon that the comprehensive recharge coefficient of the area was small. We believe that in the low groundwater level, rainfall and irrigation water are mainly used for evaporation rather than for groundwater recharge.

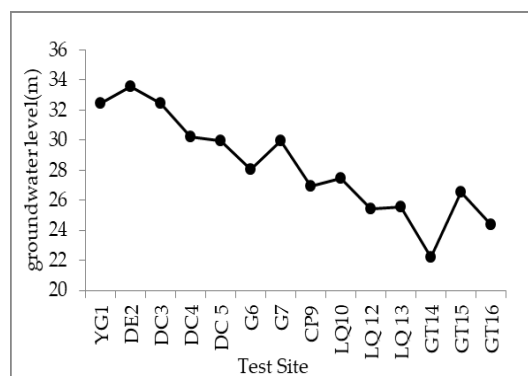


Figure 12. Groundwater level of sampling points.

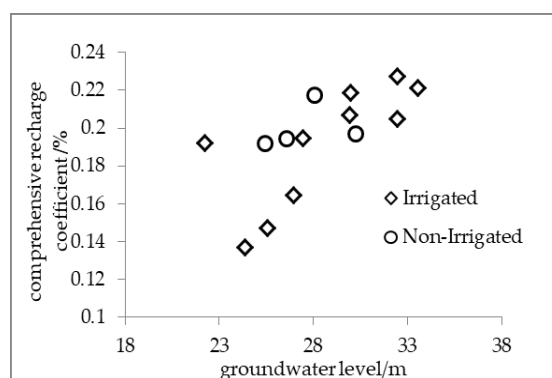


Figure 13. Correlation between groundwater level and comprehensive recharge coefficient.

3.3.4. Temporal Variability of the Recharge Rate

By comparing and analyzing the results of the two tracer tests, the average recharge rates of February–July 2015 (196 mm/a) were greater than that of July 2015–May 2016 (153 mm/a). This is mainly due to the fact that the first test interval of 168 days occurred during the period of spring irrigation and flood irrigation with more concentrated precipitation and surface water irrigation, which resulted in a larger infiltration of groundwater recharge. While in the second test interval of 286 days, the precipitation and the irrigation are more dispersed, which led to less recharge of the groundwater. The recharge rate of the first test is 20% higher than that of the second time on average, and the results in this study are consistent with those of Shuai et al. [41]. It is shown that this tracer test is reliable.

3.3.5. Comparison of Groundwater Recharge Results by Tracer Method

Considering the similar experimental methods, the tracer results in other places (North China Plain) near the research area were compared with ours in the Weishan Irrigated District. Table 6 summarized some recharge coefficient determined by tracing by other authors. The statistical results showed that the average recharge coefficient in this paper is 0.19%, which is relatively close to the 0.15% calculated by other authors. The results of this study have many experimental points and high reliability, which is of great reference value for the calculation of groundwater recharge in the Weishan Irrigated District.

Table 6. Recharge coefficient calculated by injected tracer in other places.

References	Location	Tracer Type	Number of Sites	R_c (%)
Shuai et al. [41]	North China Plain	Br^-	19	0.124
Tan et al. [32]	Piedmont Aggraded Valley Plain and Median Plain of the North China Plain	Br^-	31	0.185
Wang et al. [10]	North China Plain	^3H , Br^-	39	0.192
Liu et al. [42]	Hutuo River alluvial-proluvial fan	^3H , Br^-	3	0.160–0.180
Lin et al. [43]	Shanxi province	^3H	1	0.120
average				0.150

4. Conclusions

By comparing the obtained data of other researchers near the research area (North China Plain), this study indicates that the tracer test results can be used for the preliminary study of groundwater recharge characteristics in the Weishan Irrigated District. Average recharge rates and recharge coefficients determined by bromide tracing for different sites in the Weishan Irrigated District from 2015 to 2016 were 85.5–243 mm/a and 13.7–22.4%, respectively. By measuring bromine concentration at different sampling locations, we can conclude that the variation in the recharge rates and recharge coefficient reflects the irrigation district locations, different crops, and irrigation regimes. (1) The recharge rate of the upstream district was greater than the downstream district, which is mainly due to the difference in soil texture. The coarser the soil texture is, the greater the recharge of precipitation and irrigation water to the ground; (2) Irrigation resulted in more recharge compared to non-irrigation, which is mainly because the utilization rate of irrigation water in irrigated cropland is low; (3) Different crop types resulted in different recharge rates. Under certain conditions, the recharge rate for winter wheat-summer maize was greater than that for cotton, mainly due to the vastly different water use coefficient of these crops.

A certain positive correlation was found between the groundwater level and comprehensive recharge coefficient at the higher groundwater level. But rainfall and irrigation water are mainly used for evaporation rather than for groundwater recharge at the higher groundwater level. At the time, the correlation between them is also affected. Recharge rates estimated from the first year of tracer travel were greater than those from the second year. This difference results in part from the periodicity of total precipitation and irrigation.

Based on the above, we recommend that the irrigation area allocate and use water resources according to the irrigation time, the actual precipitation, and the groundwater level. Water resources of the Yellow River are heavily utilized during the irrigation period, thereby we can reduce the surface water resources and make rational use of the groundwater resources in the upstream and middle reaches with relatively high groundwater level. In particular, it must be noted that we should intensify the management of groundwater resources to avoid secondary salinization in some areas of the YG that might be caused by the high groundwater level. In the lower reaches of the Weishan Irrigated District with shallow groundwater, the utilization of surface water can be appropriately increased for agricultural irrigation and social production to reduce groundwater exploitation. In the flood season, the supply of groundwater increased with the increase of precipitation. At this time, the groundwater can be properly exploited to meet the needs of agriculture and social development. In other months, the utilization volume of the groundwater can be reduced. We suggest that more surface water resources, such as river water and reclaimed water, become the main water supply source in order to restore the underground water and alleviate the secondary disasters caused by the overexploitation of groundwater. It must be noted that applications of the sprinkler irrigation technique to local conditions can play an important role in providing higher water efficiency.

Further study needs to determine the recharge rates for more sites and over a longer period of time, strengthening the monitoring of variables in the potential season. Moreover, improving the testing precision of bromine can effectively improve the evaluation accuracy.

Author Contributions: All authors contributed to the design and development of this manuscript. X.C. carried out the data analysis and prepared the first draft of the manuscript; Z.X. and T.W. provided important advice on the concept, method, and structuring of the manuscript. All authors read and approved the final manuscript.

Funding: This research funding was provided by the National Sci-Tech Support Plan (grant No. 2012BAD08B05 and 2015BAD20B02), the Shandong Province Water Conservancy Research and Technology Promotion Projects (grant No. SDSLKY201410).

Acknowledgments: Many thanks to Teacher Helian Li at the University of Jinan for their assistance with Language modification, and the editors and anonymous reviewers who have given constructive suggestions on versions of this manuscript.

Conflicts of Interest: The authors declare no conflict of interest.

References

- Sanford, W. Recharge and groundwater models: An overview. *Hydrogeol. J.* **2002**, *10*, 110–120. [[CrossRef](#)]
- Wada, Y.; Beek, L.P.; Kempen, C.M.; Reckman, J.W.; Vasak, S.; Bierkens, M.F. Global depletion of groundwater resources. *Geophys. Res. Lett.* **2010**, *37*, 114–122. [[CrossRef](#)]
- Liu, Y.; Jiang, X.; Zhang, G.; Xu, Y.J.; Wang, X.; Qi, P. Assessment of shallow groundwater recharge from extreme rainfalls in the Sanjiang plain, northeast China. *Water* **2016**, *8*, 440. [[CrossRef](#)]
- Esteller, M.V.; Diaz-Delgado, C. Environmental effects of aquifer overexploitation: A case study in the highlands of Mexico. *Environ. Manag.* **2001**, *29*, 266–278. [[CrossRef](#)]
- Liu, C.M.; Yu, J.J.; Eloise, K. Groundwater Exploitation and Its Impact on the Environment in the North China Plain. *Water Int.* **2001**, *26*, 265–272.
- Allison, G.B.; Hughes, M.W. The use of natural tracers as indicators of soil-water movement in a temperate semi-arid region. *Hydrogeol. J.* **1983**, *60*, 157–173. [[CrossRef](#)]
- Gates, J.B.; Edmunds, W.M.; Ma, J.; Scanlon, B.R. Estimating groundwater recharge in a cold desert environment in northern China using chloride. *Hydrogeol. J.* **2008**, *16*, 893–910. [[CrossRef](#)]
- Scanlon, B.R.; Healy, R.W.; Cook, P.G. Choosing appropriate techniques for quantifying groundwater recharge. *Hydrogeol. J.* **2002**, *10*, 18–39. [[CrossRef](#)]
- Rueedi, J.; Purtschert, R.; Brennwald, M.S.; Hofer, M.; Kipfer, R. Estimating amount and spatial distribution of groundwater recharge in the jullemeden basin (Niger) based on 3H , 3He and CFC-11 measurements. *Hydrol. Process.* **2010**, *19*, 3285–3298. [[CrossRef](#)]
- Wang, B.G.; Jin, M.; Nimmo, J.R.; Yang, L.; Wang, W. Estimating groundwater recharge in Hebei plain, china under varying land use practices using tritium and bromide tracers. *J. Hydrol.* **2008**, *356*, 209–222. [[CrossRef](#)]
- Dogramaci, S.; Skrzypek, G.; Dodson, W.; Grierson, P.F. Stable isotope and hydrochemical evolution of groundwater in the semi-arid hamersley basin of sub-tropical northwest Australia. *J. Hydrol.* **2012**, *475*, 281–293. [[CrossRef](#)]
- Scanlon, B.R.; Keese, K.E.; Flint, A.L.; Flint, L.E.; Gaye, C.B.; Edmunds, W.M. Global synthesis of groundwater recharge in semiarid and arid regions. *Hydrol. Process.* **2010**, *20*, 3335–3370. [[CrossRef](#)]
- Beyer, M.; Jackson, B.; Daughney, C.; Morgenstern, U.; Norton, K. Use of hydrochemistry as a standalone and complementary groundwater age tracer. *J. Hydrol.* **2016**, *543*, 127–144. [[CrossRef](#)]
- Bonner, R.; Aylward, L.; Harley, C.; Kappelmeyer, U.; Sheridan, C.M. Heat as a hydraulic tracer for horizontal subsurface flow constructed wetlands. *J. Water Process Eng.* **2017**, *16*, 183–192. [[CrossRef](#)]
- Moeck, C.; Radny, D.; Auckenthaler, A.; Berg, M.; Hollender, J.; Schirmer, M. Estimating the spatial distribution of artificial groundwater recharge using multiple tracers. *Isotopes Environ. Health Stud.* **2017**, *53*, 484–499. [[CrossRef](#)] [[PubMed](#)]
- Drivas, P.J.; Shair, F.H. A tracer study of pollutant transport and dispersion in the Los Angeles area. *Atmos. Environ.* **1974**, *8*, 1155–1163. [[CrossRef](#)]

17. Hulla, J.; Bednárová, E.; Plško, J.; Kostolanský, M.; Robertson, P.K.; Mayne, P.W. Tracer methods for groundwater flow and pollution transport characterization. In *Geotechnical Site Characterization: Volume 1, Proceedings of the First International Conference on Site Characterization—ISC'98, Atlanta, GA, USA, 19–22 April 1998*; Elsevier: New York, NY, USA, 1998; Volume 4, pp. 19–22.
18. Herczeg, A.L.; Leaney, F.W. Review: Environmental tracers in arid-zone hydrology. *Hydrogeol. J.* **2011**, *19*, 17–29. [[CrossRef](#)]
19. Sukhija, B.S.; Reddy, D.V.; Nagabhushanam, P.; Hussain, S.; Giri, V.Y.; Patil, D.J. Environmental and injected tracers methodology to estimate direct precipitation recharge to a confined aquifer. *J. Hydrol.* **1996**, *177*, 77–97. [[CrossRef](#)]
20. Zimmermann, U.; Münnich, K.O.; Roether, W.; Kreutz, W.; Schubach, K.; Siegel, O. Tracers determine movement of soil moisture and evapotranspiration. *Science* **1966**, *152*, 346–347. [[CrossRef](#)] [[PubMed](#)]
21. Sukhija, B.S. Evaluation of groundwater recharge in semi-arid region of India using environmental tritium. In *Proceedings of the Indian Academy of Sciences—Section A*; Springer: Chennai, India, 1973; Volume 77, pp. 279–292.
22. Chand, R.; Chandra, S.; Rao, V.A.; Singh, V.S.; Jain, S.C. Estimation of natural recharge and its dependency on sub-surface geoelectric parameters. *J. Hydrol.* **2004**, *299*, 67–83. [[CrossRef](#)]
23. Porro, I.; Wierenga, P.J. Transient and steady-state solute transport through a large unsaturated soil column. *Groundwater* **2010**, *31*, 193–200. [[CrossRef](#)]
24. Mayes, M.A.; Jardine, P.M.; Mehlhorn, T.L.; Bjornstad, B.N.; Ladd, J.L.; Zachara, J.M. Transport of multiple tracers in variably saturated humid region structured soils and semi-arid region laminated sediments. *J. Hydrol.* **2003**, *275*, 141–161. [[CrossRef](#)]
25. Öhrström, P.; Hamed, Y.; Persson, M.; Berndtsson, R. Characterizing unsaturated solute transport by simultaneous use of dye and bromide. *J. Hydrol.* **2004**, *289*, 23–35. [[CrossRef](#)]
26. Wang, K.; Zhang, R. Heterogeneous soil water flow and macropores described with combined tracers of dye and iodine. *J. Hydrol.* **2011**, *397*, 105–117. [[CrossRef](#)]
27. Flint, A.L.; Flint, L.E.; Kwicklis, E.M. Estimating recharge at Yucca Mountain, Nevada, USA: Comparison of methods. *Hydrogeol. J.* **2002**, *10*, 180–204. [[CrossRef](#)]
28. Rice, R.C.; Bowman, R.S.; Dan, B.J. Percolation of water below an irrigated field. *Soil Sci. Soc. Am. J.* **1986**, *50*, 855–859. [[CrossRef](#)]
29. Rangarajan, R.; Athavale, R.N. Annual replenishable ground water potential of India—An estimate based on injected tritium studies. *J. Hydrol.* **2000**, *234*, 38–53. [[CrossRef](#)]
30. Müller, T.; Osenbrueck, K.; Strauch, G.; Pavetich, S.; Al-Mashaikhi, K.S.; Herb, C. Use of multiple age tracers to estimate groundwater residence times and long-term recharge rates in arid southern Oman. *Appl. Geochem.* **2016**, *74*, 67–83. [[CrossRef](#)]
31. Wu, Q.H.; Zhang, W.; Lin, W.J.; Zhang, F.W.; Wang, G.L. The Estimation of Groundwater Recharge and Preferential Flow Based on the Applied Tracers: A Case Study of Luancheng and Hengshui Areas in Hebei Province. *Acta Geosci. Sin.* **2014**, *34*, 495–502.
32. Tan, X.; Yang, J.; Song, X.; Zha, Y. Estimation of groundwater recharge in north china plain. *Adv. Water Sci.* **2013**, *24*, 73–81. (In Chinese)
33. Joshi, B.; Maulé, C. Simple analytical models for interpretation of environmental tracer profiles in the vadose zone. *Hydrol. Process.* **2015**, *14*, 1503–1521. [[CrossRef](#)]
34. Gundogdu, K.S.; Guney, I. Spatial analyses of groundwater levels using universal kriging. *J. Earth Syst. Sci.* **2007**, *116*, 49–55. [[CrossRef](#)]
35. Vucic, N. Influence of soil structure on infiltration and pF values of chernozem and chernozemlike dark meadow soils. In *Water in the Unsaturated Zone Proc Wageningen Symp*; Food and Agriculture Organization of the United Nations: Rome, Italy, 1969; pp. 344–350.
36. Zhang, L.Z.; Cao, W.X.; Zhang, S.P.; Zhou, Z.G. Characterizing root growth and spatial distribution in cotton acta phytocologica sinica. *J. Plant Ecol.* **2005**, *2*, 266–273. (In Chinese)
37. Wang, Q.X.; Wang, P.; Yang, X.Y.; Zhai, Z.X.; Wang, X.L.; Shen, L.X. Effects of Nitrogen Application Time on Root Distribution and Its Activity in Maize. *Sci. Agric. Sin.* **2003**, *36*, 1469–1475. (In Chinese)
38. Allocca, V.; Manna, F.; De Vita, P. Estimating annual groundwater recharge coefficient for karst aquifers of the southern Apennines (Italy). *Hydrol. Earth Syst. Sci.* **2014**, *18*, 56–62. [[CrossRef](#)]

39. Owor, M.; Taylor, R.G.; Tindimugaya, C.; Mwesigwa, D.; Bovolo, C.I.; Parkin, G. Rainfall intensity and groundwater recharge: Empirical evidence from the upper Nile basin. *Environ. Res. Lett.* **2009**, *4*, 035009. [[CrossRef](#)]
40. Meng, S.; Liu, J.; Zhang, Z. Spatiotemporal evolution characteristics study on the precipitation infiltration recharge over the past 50 years in the North China Plain. *J. Earth Sci.* **2015**, *26*, 416–424. [[CrossRef](#)]
41. Shuai, P.; Shi, L.S.; Cai, S.Y.; Yang, J.Z. Application of bromide tracer on estimating groundwater recharge in north China plain. *J. Irrig. Drain.* **2014**, *33*, 11–16. (In Chinese)
42. Liu, J.; Chen, Z.Y.; Zhang, Z.J. Estimation of natural groundwater recharge in the Hutuo river alluvial-proluvial fan using environmental tracers. *Geol. Sci. Technol. Inf.* **2009**, *28*, 114–118. (In Chinese)
43. Lin, R.; Wei, K. Tritium profiles of pore water in the Chinese loess unsaturated zone: Implications for estimation of groundwater recharge. *J. Hydrol.* **2006**, *328*, 192–199. (In Chinese) [[CrossRef](#)]



© 2018 by the authors. Licensee MDPI, Basel, Switzerland. This article is an open access article distributed under the terms and conditions of the Creative Commons Attribution (CC BY) license (<http://creativecommons.org/licenses/by/4.0/>).